

Heat Transfer and Entropy Generation for Natural Convection by Adiabatic Obstacles Inside a Cavity Heated on the Left Side

Jamal Baliti

Sultan Moulay Slimane university
Beni Mellal
Morocco

Mohamed Hssikou

Ibn Zohr university, Agadir
Morocco

Youssef Elguennouni

Moulay Ismail university, Meknes
Morocco

Ahmed Moussaoui

Moulay Ismail university, Meknes
Morocco

and Mohammed Alaoui

Moulay Ismail university, Meknes
Morocco

By using finite difference method, the problem of heat transfer and entropy generation for natural convection of a fluid inside a square cavity with inner adiabatic bodies has been investigated numerically. Calculations have been made for Rayleigh numbers ranging from 10^2 to $5 \cdot 10^4$ for two obstacles with different heights. Results are presented as streamlines, isotherm contours and Nusselt number for Prandtl number of 0.71 (assuming the cavity is filled with air). The obtained results demonstrate the effects of pertinent parameters on the fluid flow, thermal fields and heat transfer inside the cavity. The results show that the heat transfer rates generally increase with the shrink of the obstacle size and with the increase of Rayleigh number. The entropy generation is higher at locations with large temperature gradients. Excellent agreement is obtained with previous results in the literature.

Keywords: natural convection, cavity, entropy generation, adiabatic obstacle.

1. INTRODUCTION

Natural convection heat transfer phenomena inside cavities have been and continue to be the subject of many research activities over the past decades. It has extensive applications in different environmental situations and industrial processes with many engineering fields such as ventilation of buildings with radiators, double-glazed windows, solar collectors, cooling of electronic equipment, thermal storages and drying technologies [1]. Very intense reviews are available [2-4]. In engineering, the look is constantly focusing on the methods to enhance the overall heat transfer efficacy in a lot of applications by the realization of a wide range of techniques from design optimization to the use of new materials [5]. Yet, it is evident that the accuracy of thermal systems will be affected by fluid flow irreversibility and heat transfer irreversibility. For that, to optimize the efficiency of the system, the systems irreversibility must be checked and minimized [6]. There are numerous optimization methods to achieve this goal, among them the entropy generation minimization where reviews are available [6].

The coupling between the fluid and thermal transport phenomena often complicates the physics governing such buoyancy driven flow. Heat transfer inside a cavity with an obstacle at the centre has pertinence in modeling of baffle as a heat transfer controlling device [7], and controlling the heat rate by the aspect ratio of the adiabatic obstacle [8]. For the

purpose of determining the thermal conductivity and Reynolds number effect on the core region and velocity fields, the problem of mixed convection flow and heat transfer in a shallow enclosure with a series of block-like heat generating component [9], and the inclination effect in a square cavity containing a conduction block [10] are studied. Using finite element method, natural convection heat transfer enhancement is investigated in a cavity using a heat-conducting horizontal circular cylinder [11] and adiabatic block [12]. The effects of arc-shaped partitions, in the corners of a shallow cavity on characteristic parameters of natural convection heat transfer and fluid flow is studied using The finite volume approach [13]. Also, the effect of obstacle positions on the heat transfer and entropy generation is investigated numerically using finite difference method [14]. Entropy generation in flows is studied for different nanofluids, with silver and copper nanoparticles [15], employing innovative turbulator [16] and inside a single slope solar still [17].

Based on literature reviews, there is a large number of numerical studies on natural convection of different fluids inside enclosures with different boundary conditions, but few of them are focusing on natural convection in cavities with an inside adiabatic obstacle. In this work, the problem of natural convection heat transfer, fluid flow and heat generation in a square enclosure containing air and with two thin adiabatic obstacles located at its inside and with a fixed temperature drop between the vertical walls, is investigated by finite difference method based. The results in the form of streamlines, entropy rate contours and isotherms plots and average Nusselt number are presented for a wide range of Rayleigh numbers and size and location of the adiabatic thin obstacles. Com-

Received: May 2020, Accepted: July 2020

Correspondence to: Jamal Baliti

Polydisciplinary faculty, Sultan moulay Slimane university, Beni Mellal, Morocco.

E-mail: jamal.baliti@usms.ma

doi: 10.5937/fme2004825B

© Faculty of Mechanical Engineering, Belgrade. All rights reserved

FME Transactions (2020) 48, 825-832 825

parison of the present results with previous numerical data are also presented.

2. PHYSICAL MODEL

2.1 Problem statement

In this study, we consider heat transfer and entropy generation in a square cavity, characterized by a length W with a heated left plate and filled with a viscous fluid. The heated surface is taken to T_H , and the right surface is taken to the environmental temperature T_C and the two other surfaces are assumed to be adiabatic. Inside the enclosure there are two adiabatic obstacles fixed at the horizontal walls. They are characterised by the height h and distance from the left plate by L and l respectively (fig.1).

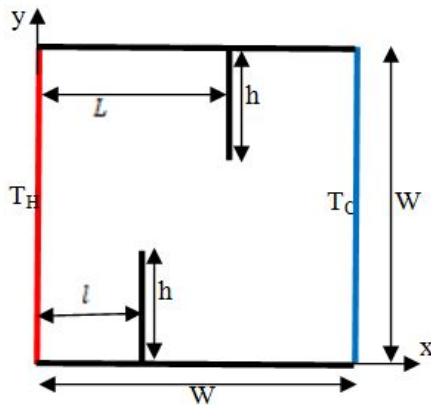


Figure 1. Geometry and prescribed plate temperatures for the cavity.

2.2 Governing equations

In this work the fluid is considered as a Newtonian fluid with constant properties apart from density in the momentum equation for body force term. Incompressible flow with thermal convection is assumed in its steady state. The Boussinesq approximation, which relates the density changes to the temperature variations, assumes that variations in density have no effect on the flow field, except that they give rise to buoyancy forces thus couples temperature-field with the flow field. Radiation and heat production in the cavity domain is negligible and the gravity acts in the vertical direction. The governing equations for the natural convection flow with conservation of mass, momentum and energy can be written as [8]:

$$\frac{\partial u}{\partial x} + \frac{\partial v}{\partial y} = 0 \quad (1)$$

$$u \frac{\partial u}{\partial x} + v \frac{\partial u}{\partial y} = \frac{1}{\rho} \left[-\frac{\partial p}{\partial x} + \mu \left(\frac{\partial^2 u}{\partial x^2} + \frac{\partial^2 u}{\partial y^2} \right) \right] \quad (2)$$

$$u \frac{\partial v}{\partial x} + v \frac{\partial v}{\partial y} = \frac{1}{\rho} \left[-\frac{\partial p}{\partial y} + \mu \left(\frac{\partial^2 v}{\partial x^2} + \frac{\partial^2 v}{\partial y^2} \right) + \rho g \beta (T - T_C) \right] \quad (3)$$

$$u \frac{\partial T}{\partial x} + v \frac{\partial T}{\partial y} = \alpha \left(\frac{\partial^2 T}{\partial x^2} + \frac{\partial^2 T}{\partial y^2} \right) \quad (4)$$

where u and v are the velocity components in the x and y directions respectively, T represents the temperature, p and ρ depict the pressure and density respectively, g represents the gravity magnitude and μ and α represent the viscosity and thermal diffusion. The governing equations can be given in dimensionless form, by applying the dimensionless variable as follows:

$$x' = \frac{x}{W}, y' = \frac{y}{W}, l' = \frac{l}{W}, L' = \frac{L}{W}, h' = \frac{h}{W}, u' = \frac{uW}{\alpha}, v' = \frac{vW}{\alpha}, p' = \frac{pW^2}{\rho\alpha^2}, \theta = \frac{T - T_C}{\Delta T}, Pr = \frac{\nu}{\alpha} \text{ and } Ra = \frac{g\beta W^3 \Delta T}{\nu\alpha}$$

where $x', y', l', h', u', v', p'$ and θ are the dimensionless variables and Pr and Ra are respectively the Prandtl and Rayleigh numbers. The dimensionless form of the governing equations -where the apostrophe has been dropped for the sake of clarity- is obtained easily with these non-dimensional variables as [12]:

$$\frac{\partial u}{\partial x} + \frac{\partial v}{\partial x} = 0 \quad (5)$$

$$u \frac{\partial u}{\partial x} + v \frac{\partial u}{\partial y} = -\frac{\partial p}{\partial x} + Pr \left(\frac{\partial^2 u}{\partial x^2} + \frac{\partial^2 u}{\partial y^2} \right) \quad (6)$$

$$u \frac{\partial v}{\partial x} + v \frac{\partial v}{\partial y} = -\frac{\partial p}{\partial y} + Pr \left(\frac{\partial^2 v}{\partial x^2} + \frac{\partial^2 v}{\partial y^2} \right) + Pr Ra \theta \quad (7)$$

$$u \frac{\partial \theta}{\partial x} + v \frac{\partial \theta}{\partial y} = \left(\frac{\partial^2 \theta}{\partial x^2} + \frac{\partial^2 \theta}{\partial y^2} \right) \quad (8)$$

The stream function is defined based on the continuity equation as follows [11]:

$$u = \frac{\partial \psi}{\partial y} \text{ and } v = -\frac{\partial \psi}{\partial x} \quad (9)$$

The rate of heat transfer across the walls of the enclosure was calculated using a wall surface Nusselt number (Nu), which is defined as the ratio of convective heat transfer to pure conduction across the boundary, along the heated wall of the cavity. The local Nusselt number and the averaged one along the upper wall of the cavity are expressed by,

$$Nu_{loc} = -\frac{\partial \theta}{\partial y} \quad (10)$$

$$Nu = \int_0^1 Nu_{loc} dx \quad (11)$$

2.3 Boundary conditions

To solve equations (5)-(11) one must have some boundary conditions. The problem is subjected to no-slip boundary condition on the walls, i.e. $u=v=0$ on both four walls of the cavity and the obstacles. the following are the thermal boundary conditions are as follows:

- $\frac{\partial \theta}{\partial y} = 0$ on the horizontal walls,
- $\frac{\partial \theta}{\partial x} = 0$ on the obstacles,

- $\theta = 1$ on the left wall and
- $\theta = 0$ on the right wall.

2.4 Entropy generation

Based on the thermodynamic equilibrium of linear transport theory, the entropy generation for fluid flow is given as [6,18]:

$$S = S_h + S_f \quad (12)$$

where S_h is the irreversibility due to heat transfer in the direction of finite temperature gradients, and S_f is the contribution of fluid friction irreversibility to the total generated entropy [18]. These two functions are written in terms of the primitive variables as [6]:

$$S_h = \left(\frac{\partial \theta}{\partial x} \right)^2 + \left(\frac{\partial \theta}{\partial y} \right)^2 \quad (13)$$

$$S_f = \Phi \left[4 \left(\frac{\partial^2 u}{\partial x \partial y} \right) + \left(\frac{\partial u}{\partial y} + \frac{\partial v}{\partial x} \right)^2 \right] \quad (14)$$

where $\Phi = \frac{\mu T_C \alpha^2}{kW^2 \Delta T^2}$ is the irreversibility distribution ratio, with $\Delta T = T_H - T_C$.

3. NUMERICAL METHOD

The governing equations are solved numerically by finite difference methods using the Gauss-Seidel technique with a house Fortran code. The governing equations are discretized by applying second order accurate central difference schemes and the discretized equations obtained were solved iteratively. The iterative calculus is launched by the velocity field followed by the energy equation solution and is continued until convergence is achieved. Convergence is attained by the sum of the absolute relative errors for each dependent variable in the entire flow field:

$$\sum_{i,j} \frac{|\phi_{i,j}^{n+1} - \phi_{i,j}^n|}{|\phi_{i,j}^{n+1}|} < \varepsilon \quad (16)$$

where, the superscript n refers to the iteration number, ϕ represents the variables u , v or θ and the subscripts i and j refer to the coordinates in an x and y directions. The value of ε is chosen as $\varepsilon = 10^{-5}$ for all calculations.

3.1 Validation

To make sure of the validity and to verify the accuracy of the used numerical technique, the outcomes for Nusselt number are compared with the solution of Oztop et al.[14] for a fluid of $Pr = 0.71$ in a square cavity with top and bottom adiabatic plates, while the two others are taken cold with a heated obstacle inside. Another comparison is made with Famouri et al. [18]. In his work, the cavity is filled with the air and have an inside heated obstacle with two side cold walls, while the top and bottom are insulated. Figure.2a-b show these

two comparisons respectively which describe an excellent agreement between the present results and the presented solution for different values of Ra . The comparison takes on the averaged Nu along the hot wall. Also, a third comparison is made between the considered method and benchmark of solutions for a square enclosure, confining the air, with a heated left side without any obstacle inside. The comparison (Table.1) is taken for a lot of Ra numbers to calculate the Nu number and the results match very well with previously published results given by the refs [19-22].

Table 1. Comparison of averaged Nusselt number with previous works for a square cavity without obstacle and various Ra numbers.

Nu	Present work	Ridouane et al. [19]	Barakos et al. [20]	Davis [21]	Fusegi et al. [22]
50	1.010	1.000	-	-	-
$5 \cdot 10^2$	1.044	1.036	-	-	-
10^3	1.128	1.121	1.114	1.118	1.105
10^4	2.264	2.273	2.245	2.243	2.302
10^5	4.521	4.586	4.510	4.519	4.646
10^6	8.991	9.012	8.806	8.799	9.01

3.2 Grid independency

The solution was considered to be fully converged when the maximum absolute values of the dependent variables at any node from iteration to iteration are smaller than a prescribed value, chosen as 10^{-5} . The numerical solutions were conducted using a two-dimensional grid with 121×121 uniformly spaced grid points. A grid independence test was conducted with different meshes of size $N = 33, 41, 61, 81, 101, 121, 141, 161$ and 201 . Figure 3 a shows, for various mesh sizes, the relative change in the averaged Nusselt number from the upper surface. The maximum deviations observed in terms of Nu within 0.39% and 0.23% , when the grid of 101×101 and 121×121 are considered respectively (Figure 3b). This justifies the selected grid size of 121×121 as a reasonable compromise between computational effort and required accuracy.

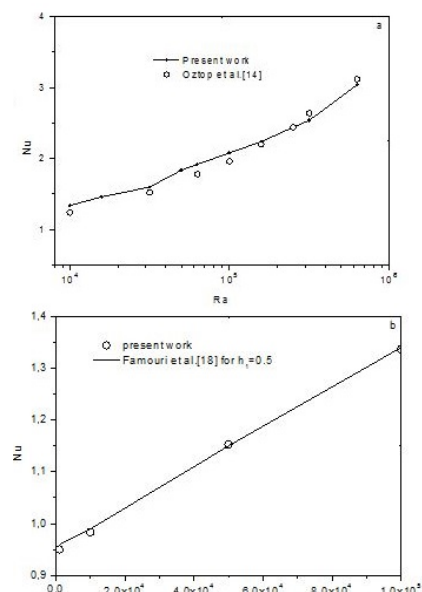


Figure 2. Code verification with the results of a) Oztop et al. [14] and b) Famouri et al.[18]

4. RESULTS

Heat transfer and entropy generation for natural convection inside a square cavity heated in the side wall with two adiabatic obstacles are considered. The effect of the two obstacles fixed in the adiabatic plates with different positions and separate distances is examined in this study. The study is conducted for Rayleigh number, Ra , from 10^2 to $5 \cdot 10^4$.

4.1 Heat transfer

Figures 4 show the streamlines and isotherms obtained for different heights of the obstacles located at the centre of the two horizontal plates, $L = l = 1/2$, for all Rayleigh numbers; $Ra = 10^2, 10^4, 5 \cdot 10^4$. The initial rise and drop of air temperature (temperature here and after means dimensionless temperature) at the vicinity of the heated plate begin by conduction mechanism of heat transfer. Later, owing to the appearance of a temperature difference inside the cavity, the heat transfer mechanism is changed to natural convection that induces flow movement.

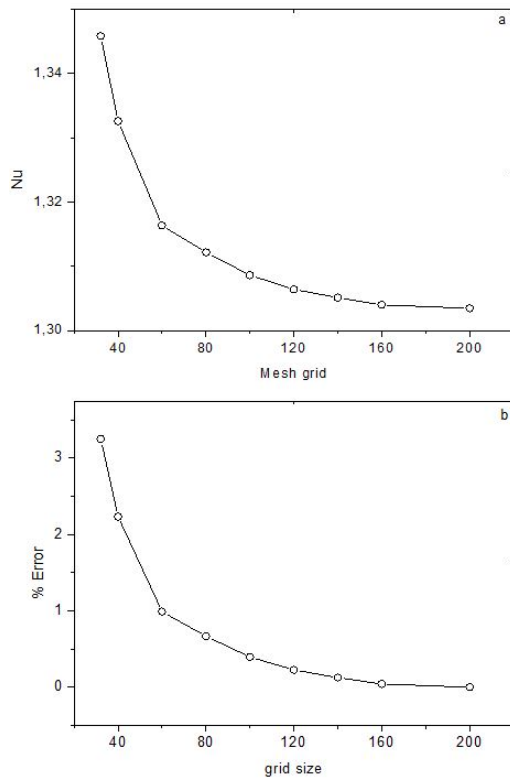
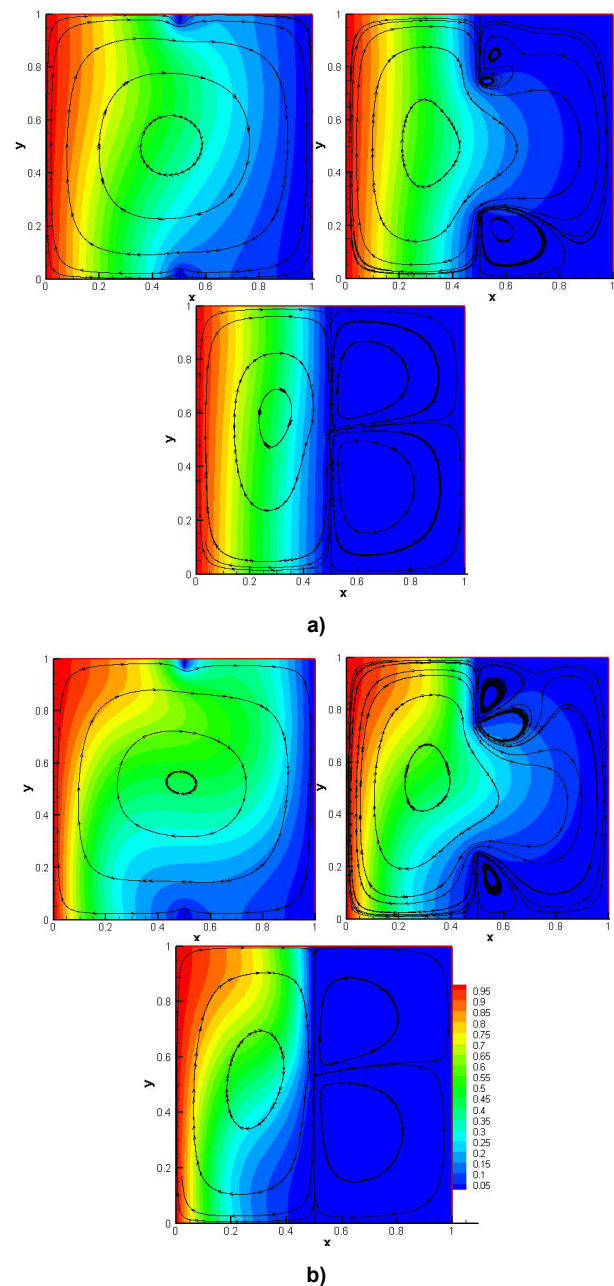


Figure 3. Grid independence test of the numerical solution in terms of average Nusselt number.

It is observed that when the separate distance between the two obstacles is big, i.e. small obstacles height, only one cell is formed in the cavity for all Rayleigh numbers. The fluid motion in this case is symmetric for the small Rayleigh number due to conduction mechanism dominance. By increasing the Rayleigh number the convection becomes dominant over the conduction and the motion symmetry breaks down. When the inside plates get closer to each other, $h = 1/4$, one vortex is created in the left part of the cavity. While, three other cells are observed in right one; two near the top obstacle and one about the

downone. As Rayleigh number increases, the two eddies, top and bottom, become stronger and the medium one becomes more and more smaller. The height growth of the two obstacles to $h = 15/32$ creates the disappearance of the medium cell and the top and down vortices become stronger. It is also evident that the size of vortices in the left part of the enclosure is proportional to the height of the inside adiabatic bodies; $h = 1/4$ and $h = 15/32$. For the highest Rayleigh number, $Ra = 5 \cdot 10^4$, the effect of convection mechanism is very clear. The primary cell is subdivided into its centre to two small vortices for $h = 1/32$, while a fourth vortex is created next to the lowest obstacle for the case where $h = 1/4$.

By the increase of the height of the two inside plates, the contours of temperature become stratified from the heated plate to the two adiabatic bodies especially when Rayleigh number is smaller. By the increase of the separate distance between these two obstacles, the conduction mechanism penetrates heating into the right part of the cavity.



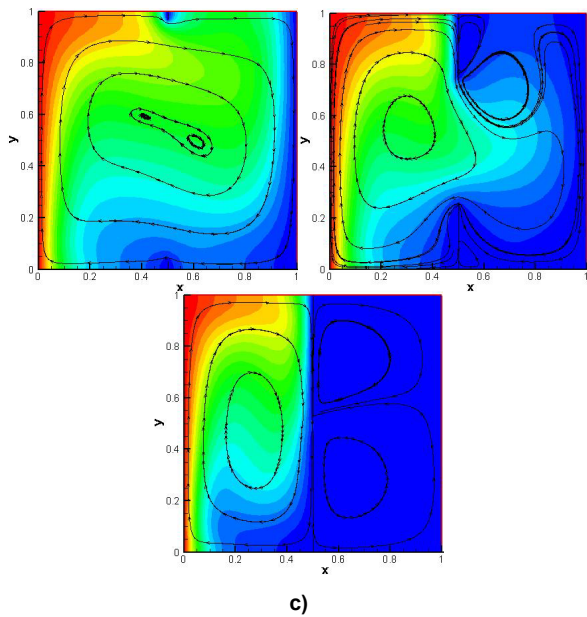


Fig.4 Streamlines overlaid isotherms for $h = 1/32, 1/4, 15/3, l = L = 1/2$ and a) $Ra = 10^3$, b) $Ra = 10^4$, c) $Ra = 5 \cdot 10^4$.

Figure 5 illustrates the streamlines and temperature contours for different obstacles height and in their respective positions $l = 1/4$ and $L = 3/4$ for $Ra = 10^4$. When the height of the inside bodies is $h=1/4$, the same number of vortices is created and there is no great change in their form. Considering the case where $h = 1/2$, the primary cell seen in Fig. 5b is divided into two vortices by the effect of the first obstacle. While the two eddies observed in the same figure next to the second obstacle gained more space inside the cavity. By increasing the adiabatic bodies' height (Fig. 5c), another eddy is created in the right part of the square enclosure. The heat inside this cavity is almost taken by the flow movement.

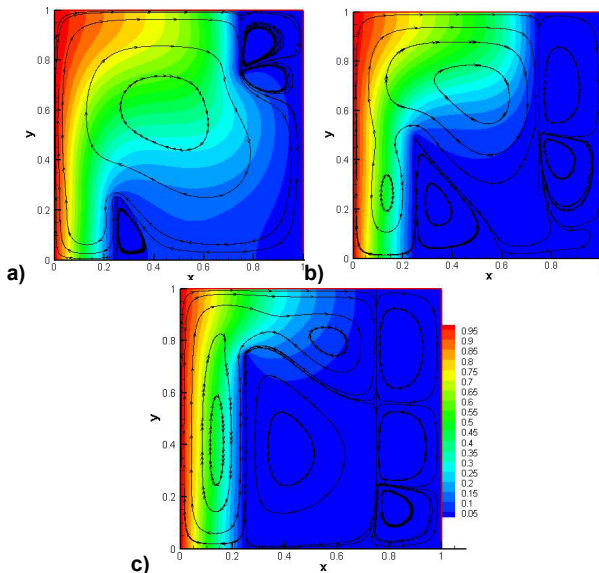


Figure 5. Streamlines overlaid isotherms for $l = 1/4, L = 3/4$ a) $h = 1$, b) $h = 1/2$, c) $h = 3/4$ and $Ra = 10^4$.

At the right parts of the cavity, the flow is induced by natural convection while the isothermal values are zero and equal to the temperature of the side walls. The increase of the obstacles height increases the cooling inside the right part of the cavity and has no great effect on the left one. It is clear in this case that, at the left

upper side of the enclosure, the fluid temperature is greater than the temperature next the obstacles, and the heat transfer direction is from the air to the inside plates. Conversely, at the right half of the cavity, the direction of heat transfer is from the obstacles to the air. The growth of the Rayleigh number has a good effect on the heat penetration inside the right part of the cavity from the opening created by the two inside bodies.

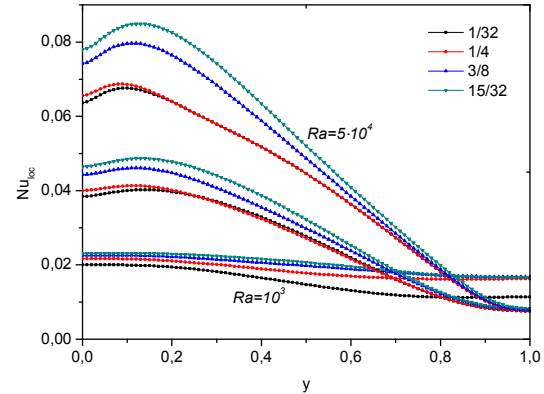


Figure 6. Local Nusselt number for different obstacles height for $L = l = 1/$ and Rayleigh number $Ra = 10^3, 10^4$ and $5 \cdot 10^4$.

Figure 6 plots the variation of local Nusselt number along the left wall for different obstacles heights at Rayleigh numbers $Ra = 10^3, 10^4$ and $5 \cdot 10^4$. When the Ra number is higher, the amount of heat added to the fluid in the left-upper region of the enclosure becomes larger, which consecutively intensifies fluid convection. In the upper region of the left plate the cold fluid that is brought there by the recirculation patterns from the lower part of the cavity is heated up. As a result, the local Nusselt number becomes higher there. The heated air from the upward of the left wall reaches the left enclosure corners, losing heat to the inside cold air, and thus the local Nusselt number becomes lower in these regions. As the obstacles height increases, the heat is prevented from penetrating inside the cavity right side which enhances the local Nusselt number.

4.2 Overall heat transfer

The overall heat transfer is pointed out in terms of mean Nusselt numbers. In figure 7a, mean Nusselt number was plotted for different height of the obstacles and at different Rayleigh numbers. As the height of the obstacles increases for fixed Ra numbers, mean Nusselt numbers increase. Besides, for constant height of obstacles, when Rayleigh numbers are increased an analogous increase of mean Nusselt number value is created. It can be observed that for low Rayleigh numbers, $Ra = 10^2$ and $= 10^3$, as Nu is quite close to unity the pure conduction heat transfer mechanism is effectively the dominant. The heat transfer rates show a large increase for the highest obstacles height at Rayleigh number values higher than 10^4 .

Fig.7b illustrates ψ_{max} for different Ra and obstacles height values. As seen, ψ_{max} values increase with obstacles height for a fixed Ra number. The effect of Rayleigh number on the intensification of the fluid circulation is evident in this figure, where as Rayleigh number is increased the ψ_{max} value is analogously increased.

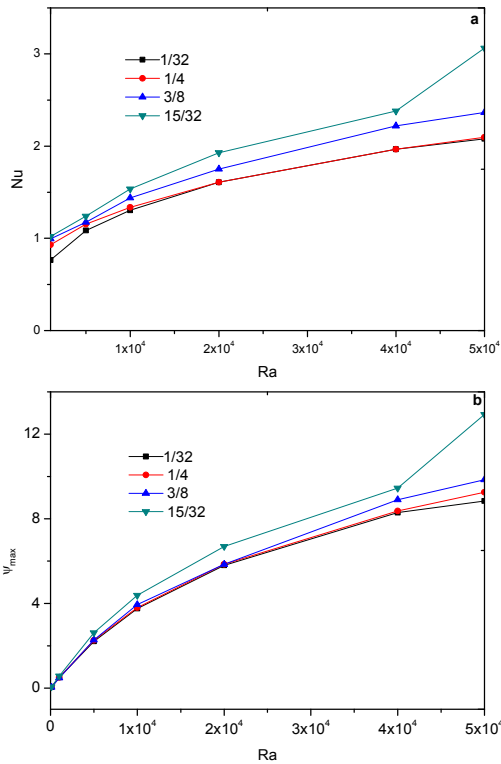


Figure 7. a)Average Nusselt number and b) Max stream function for different Rayleigh numbers, obstacles height and $L = l = 1/2$.

4.3 Entropy generation

Figure 8 reports entropy generation rate, N_s , contours inside an enclosure with two interior adiabatic bodies, with height $h = 1/4$ at different Rayleigh numbers.

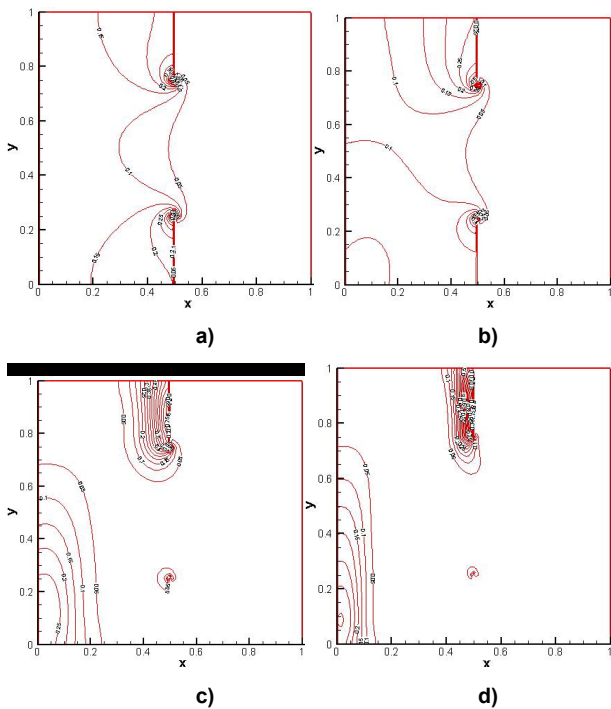


Figure 8. Entropy generation rate for $l = L = 1/2$, $h = 1/4$ and a) $Ra = 10^2$, b) $Ra = 10^3$, c) $Ra = 10^4$ and d) $Ra = 5 \cdot 10^4$.

It is worth noting that, by increasing Ra number there is more vigorous mixing and hence there are severe temperature gradients at the top left corner and a

high drop in its gradient next the right part of the enclosure ; which is proved by variations of the entropy generation rate (Fig. 8).

It is observed that, for any arrangement of the partition, the active sites of entropy production are regions close to the left side of the adiabatic inside bodies where the highest flow movement and heat flux can be detected due to the presence of the heat source, i.e. the left heated wall.

As it is seen, the entropy generation is higher at high temperature gradients. This is due to heat transfer irreversibility because large heat transfer is confined to these locations. It is clear from Fig.8 that for all cases of obstacles heights, entropy generation is mainly confined to the left side of the cavity and the adiabatic bodies, while, there is no entropy generation at the enclosure right side where there is no significant variation in the temperature. There is no great changes in the temperature profile in the cavity centreline going from $Ra = 10^2$ to $Ra = 10^3$, while the entropy generation starts its increase in the left down part of the cavity due essentially to the beginning of the convection effect.

4.4 Temperature profile

In the goal of assessing the penetration depth of the temperature boundary layer formed on the left wall of the enclosure, the temperature distribution in the middle plane of the enclosure, $y=0.5$, is shown in Figure 9. In particular, for every Rayleigh number studied, the temperature takes the unit value at the left of the middle plane of the enclosure and then decreases with increasing distances from the left wall for Rayleigh numbers till 10^4 . But, for high Ra number, $Ra = 5 \cdot 10^4$, the temperature in the middle plane decreases to $\theta_{mp,min}$ then it increases until $\theta_{mp,max}$, near the two adiabatic obstacles where it drops for the second time. These temperature variations inside the cavity are observed especially for the lowest height of the obstacles.

Table 2. Asymptotic values of middle plane temperature at $Ra = 5 \cdot 10^4$ and different h values.

h	1/4	3/8	15/32
$\theta_{mp,min}$	0,4285	0,4062	0,3476
$\theta_{mp,max}$	0,4585	0,4322	0,4256

As the opening, given by the two adiabatic obstacles, is big the temperature fronts penetrate from the left wall deeply inside the fluid body of the right part of the cavity. But, when this opening becomes smaller the temperature is affected by a sudden decrease-increase near the obstacles, which is translated by the no temperature's penetration to the right part of the enclosure until the highest Ra number; $Ra = 10^4$.

In the case of the lowest obstacles height, there is no asymptotic value of the middle-plane temperature in the core region of the enclosure. In this case the temperature is in constant decrease with x coordinates. The increase in the obstacles height causes a decrease in the asymptotic values of the middle-plane temperature in the core region, for high Rayleigh number where the dominance of convective heat transfer (TABLE 2).

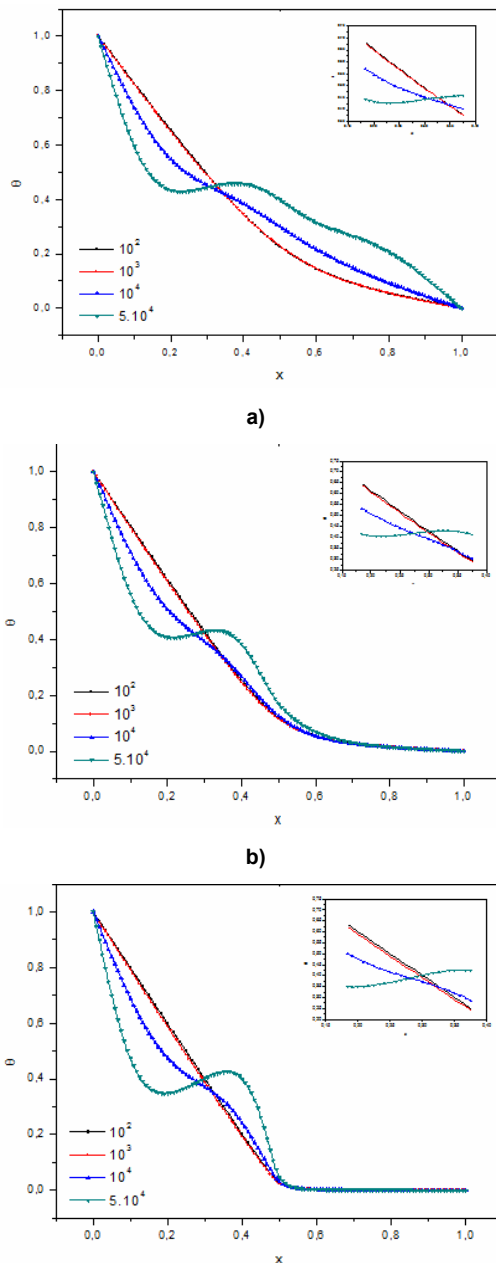


Figure 9. Temperature in the middle plane for different Rayleigh numbers and obstacles height a) $h = 1/4$, b) $h = 3$ and c) $h = 15/32$.

5. CONCLUSION

In the present study, finite difference method is applied to simulate the natural convection fluid flow, heat transfer and entropy generation of air inside a square cavity equipped with two adiabatic obstacles. The effect of the Rayleigh number, height and position of the two obstacles in the flow pattern, temperature field and the characteristics of heat transfer and entropy generation were investigated. As a result, the average Nusselt number is increased by the Rayleigh number increase for fixed obstacles height and by the inside bodies height decrease for constant Ra number. Furthermore, the high obstacles' opening allows the penetration of heat inside the right part of the cavity, which is not permitted for the lowest one. Also, for small height of inside bodies the increase of Ra number creates two vortices in the main circulation inner and develops other

eddies in the right side of the cavity for big heights. Finally, the entropy generation is higher at locations where there is higher temperature gradients, due to heat transfer irreversibility created by large confined heat transfer.

REFERENCES

- [1] Laguerre, O., Benamara, S., D.Remy, and Flick, D., *Experimental and numerical study of heat and moisture transfers by natural convection in a cavity filled with solid obstacles*, International Journal of Heat and Mass Transfer, vol. 52, pp .5691-5700, 2009.
- [2] Bejan, A., *Convection Heat Transfer*, third ed., Wiley, New York, 2005.
- [3] Khramtsou, P.P., Martyneuko, O.G., *Free Convection Heat transfer*, Springer Edition, 2005
- [4] Khalifa, A. J. N., *Natural convective heat transfer coefficient—a review: II. Surfaces in two-and three-dimensional enclosures*, Energy Conversion and Management, vol. 42(4), pp.505-517, 2001.
- [5] Khan, T. Z. and Parvin, S., *Effects of Lewis number on two phase natural convection flow of nanofluid inside a square cavity with an adiabatic obstacle*, In AIP Conference Proceedings, Vol. 2121, AIP Publishing, 2019.
- [6] Rahimi, A., Dehghan Saeed, A., Kasaeipoor A. and Hasani Malekshah, E.A *comprehensive review on natural convection flow and heat transfer: the most practical geometries for engineering applications*, International Journal of Numerical Methods for Heat & Fluid Flow, 29(3), pp. 834-877, 2019.
- [7] Karki, P. Yadav, A. K. and Perumal, D. A., *Study of Adiabatic Obstacles on Natural Convection in a Square Cavity Using Lattice Boltzmann Method*, Journal of Thermal Science and Engineering Applications, vol.11(3), 2019.
- [8] Mousa, M. M., *Modeling of laminar buoyancy convection in a square cavity containing an obstacle*, Bulletin of the Malaysian Mathematical Sciences Society, vol.39(2), pp.483-498, 2016.
- [9] Bhoite, M. T., Narasimham G. S. L. and Murthy, M. K., *Mixed convection in a shallow enclosure with a series of heat generating components*, Int. J. Thermal Sci. vol. 44, pp.125-135, 2005.
- [10] Das, M. K. and Reddy, K. S. K., *Conjugate natural convection heat transfer in an inclined square cavity containing a conducting block*, International Journal of Heat and Mass Transfer, vol. 49, pp.25-26, 2006.
- [11] Rahman M. M., Alim, M. A., and Mamun, M. A. H., *Finite element analysis of mixed convection in a rectangular cavity with a heat-conducting horizontal circular cylinder*. Nonlinear Analysis: Modelling and Control, vol.14(2), pp.217-247, 2009.
- [12] Bhave, P., Narasimhan A. and Rees, D. A. S., *Natural convection heat transfer enhancement using adiabatic block: optimal block size and Prandtl number effect*, International Journal of Heat

and Mass Transfer, vol.49(21-22), pp.3807-3818, 2006.

- [13] Gurturk, M., Oztop, H. F. Selimefendigil, F. and Al-Salem, K., *Effects of Arc-Shaped Partitions in Corners of a Shallow Cavity on Natural Convection*, Hittite Journal of Science & Engineering, vol. 6(1), pp. 17-23, 2019.
- [14] Oztop, H. F., Dagtekin I., and Bahloul, A., *Comparison of position of a heated thin plate located in a cavity for natural convection*, International communications in heat and mass transfer, vol.31(1), pp.121-132, 2004.
- [15] Hayat, T., Khan, M. I., Qayyum, S. and Alsaedi, A., *Entropy generation in flow with silver and copper nanoparticles*, Colloids and Surfaces A: Physicochemical and Engineering Aspects, vol. 539, pp.335-346, 2018.
- [16] Sheikholeslami, M., Jafaryar, M., Shafee, A., Li, Z. and Haq, R. U. *Heat transfer of nanoparticles employing innovative turbulator considering entropy generation*, International Journal of Heat and Mass Transfer, vol. 136, pp.1233-1240, 2019.
- [17] Rashidi, S., Akar, S., Bovand, M. and Ellahi, R., *Volume of fluid model to simulate the nanofluid flow and entropy generation in a single slope solar still*, Renewable Energy, vol. 115, pp. 400-410, 2018.
- [18] Famouri M. and Hooman, K., *Entropy generation for natural convection by heated partitions in a cavity*, International Communications in Heat and Mass Transfer, vol.35(4), pp.492-502, 2008.
- [19] Ridouane, E. H. and Campo, A., *Free convection performance of circular cavities having two active curved vertical sides and two inactive curved horizontal sides*, Applied thermal engineering, vol.26(17-18), pp.2409-2416, 2006.
- [20] Barakos, G., Mitsoulis, E. and Assimacopoulos, D., *Natural convection flow in a square cavity revisited: laminar and turbulent models with wall*

functions,” International Journal for Numerical Methods in Fluids, vol.18(7), pp. 695-719, 1994.

- [21] de Vahl Davis, G., *Natural convection of air in a square cavity: a bench mark numerical solution*, International Journal for numerical methods in fluids, vol. 3(3), pp. 249-264, 1983.
- [22] Fusegi, T., Hyun, J. M., Kuwahara K. and Farouk, B., *A numerical study of three-dimensional natural convection in a differentially heated cubical enclosure*, International Journal of Heat and Mass Transfer, vol.34(6), pp. 1543-1557, 1991.

**ПРЕНОС ТОПЛОТЕ И СТВАРАЊЕ
ЕНТРОПИЈЕ ЗА ПРИРОДНУ КОНВЕКЦИЈУ
ФЛУИДА АДИЈАБАТСКИМ ПРЕПРЕКАМА
УНУТАР ШУПЉИНЕ ЗАГРЕЈАНЕ НА ЛЕВОЈ
СТРАНИ ЗИДА**

**Ј. Балити, М. Хсикоу, Ј. Елгенуни, А. Мусауи,
М. Алауи**

Метода коначних разлика је коришћена за нумеричко истраживање проблема преноса топлоте и стварања ентропије за природну конвекцију флуида унутар правоугле шупљине у којој се налазе адијабатска тела. Израчунавања су вршена помоћу Рајлијевог броја $10^2 - 5 \cdot 10^4$ за две препреке различите висине. Резултати су приказани као струјнице, изотермне контуре и Нуселтов број за Прандтлов број 0,71 (под претпоставком да је шупљина испуњена ваздухом). Показано је да постоји утицај одговарајућих параметара на струјање флуида, топлотно поље и пренос топлоте унутар шупљине. Брзина преноса топлоте се повећава са смањењем димензија препреке и повећањем Рајлијевог броја. Стварање ентропије је веће на местима са већим температурним градијентом. Наши резултати се у потпуности слажу са резултатима приказаним у литератури.